

TIDAL EFFECTS ON CIRCULATION AND MIXING IN THE OMBAI STRAIT REGION

Robin Robertson *

Univ. of New South Wales at the Australian Defence Force Academy, Canberra, Australia

1. INTRODUCTION

Besides being a chokepoint in the surface return flow of the global thermohaline circulation from the Pacific Ocean to the Atlantic Ocean, the Indonesian Throughflow (ITF) region plays a key role in the regional climate of Austral-Asia and is important to shipping between the Indian and Pacific Oceans. Sea surface temperatures in the Indonesian Seas influence precipitation in the region, which impacts agricultural yields, fresh-water availability, and occurrence of bush fires and landslides (Gordon, 2005). The surface return flow of the thermohaline circulation from the Pacific flows through the ITF. The ITF outflow comprises this return flow. ITF outflow characteristics depend not only on the waters flowing in from the Pacific, but also on their transformation by the “Indonesian Mix-Master” during their passage through the Indonesian Seas (Gordon, 2005). A major factor in determining the outflow characteristics is the extent and intensity of this mixing with the primary mechanism for the “Mix-Master” believed to be tides (Gordon, 2005; Hatayama, 2004; Hatayama et al., 1996; Field and Gordon, 1996, 1992).

Ocean conditions in the Indonesian Seas have been measured by a few observational programs, notably Arlindo (Susanto et al., 2000) and INSTANT (Sprintall et al., 2004); however, due to the inherent difficulties of working in the region, observations are sparse and do not provide good coverage either spatially or temporally. To fill in the gaps, tidal simulations of the region have been made by Hatayama et al. (1996), Mazzega and Bregé (1984), Egbert and Erofeeva (2002), and Ray et al. (2005) with good result in replicating observed barotropic tidal elevations and currents. However, barotropic tides are not the entire story. Internal or baroclinic tides generated within the water column by interactions of the barotropic tide with topographic features also affect the elevation and currents and are believed to be responsible for much ocean mixing (1979). The aforementioned simulations were 2-D and did not simulate internal tides.

To evaluate effects of internal tides, baroclinic tides were simulated for the Indonesian Seas by Robertson and Field (2008) using a 3-D terrain-following, primitive equation model. The model showed extremely complex velocity fields, resulting from constructive and destructive interactions of internal tides generated in various locations (Robertson and Field 2008). These model results are the basis of this study, which will focus on a single portion of the Indonesian Sea, the Ombai Strait region. Three important new features of the circulation were identified by the model study: a strong, tidal current, which was dependent on the spring-neap tidal cycle, surface trapped tidal velocities, and strong localized upper layer mixing over Ombai Sill.

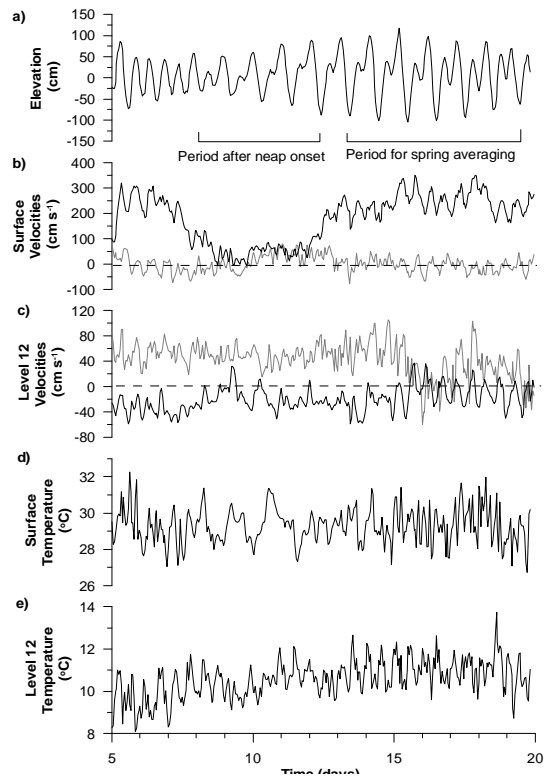


Figure 1. Time series of the a) elevation, b) surface and c) mid-water column velocities, U_3 (black) and V_3 (gray), and d) surface and e) mid-water column potential temperatures over the slope south of the sill north of Ombai Strait (340 km).

2. Ombai Jet

An extremely strong eastward current of 2-2.4 m s⁻¹ was present in the upper ocean through Ombai Strait (1 and Figure 2a) and has been nicknamed the Ombai Jet. For ~4 days after the onset of neap tide (Figure 1a), this Ombai Jet disappeared (Figure 1b and Figure 2b) and the surface layer was slightly cooler and saltier, by ~0.6°C (Figure 1d) and 0.006 psu, respectively. Below the surface layer, there were no appreciable changes in the velocities (Figure 1c), potential to the west of Ombai Strait during the spring tide period (Figure 2c). This elevation gradient was absent during the period after the onset of neap tide when the Ombai Jet was absent (Figure 2d). The current flowed southeast across the Ombai Strait transect (Figure 1a) spanning the width of the strait and the upper water column from the surface to the strong pycnocline. It opposed the mean flow of the area (Gordon 2005) and the propagation of the diurnal tide (Egbert et al. 2002; Ray et al. 2005; Robertson and Field 2008). M_2 elevations differ by >25 cm in amplitude and 45° in phase (~1.5 hrs) on the different sides of the Greater Sunda Islands where the

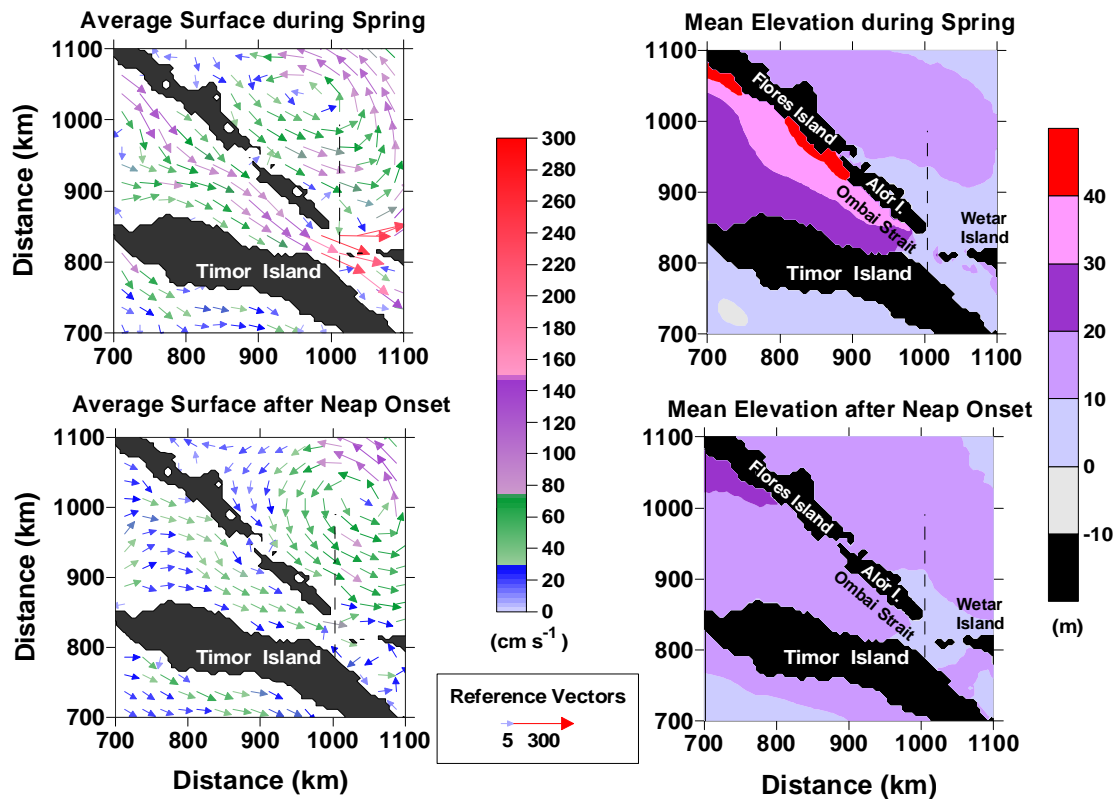


Figure 2. The average surface velocities during the periods marked in Figure 1 for a) spring tide and b) after the onset of neap tide. The average elevation during these periods c) for spring tide and d) after the onset of neap tide.

elevation gradient builds (Robertson and Field 2008). This resulted in an elevation gradient between the different sides of the Greater Sunda Islands due to the different amplitudes and stages of propagation of the tides on either side of the islands, particularly Flores Island. Since the Ombai Jet appeared only at the surface, it is believed that this elevation gradient drove flow through breaks in the island chain, particularly Flores Island, over shallow sills increasing the volume in the surface layer and providing the driving force for the surface jet. Supporting this, a large elevation gradient extends on the south side of the Greater Sunda Islands and the tides are known to have different phases and amplitudes on the different sides (Robertson and Field 2008). At neap tide, these elevation differences are smaller, reducing flow over the sill(s), which is the driving force for the jet, and allowing the jet to relax. Since the simulations only had tidal forcing and did not have currents driven by the wind or transport from the Pacific to the Indian Ocean, the Ombai Jet will be modified by these forces in observations. However, observations at a nearby mooring location showed a strong, intermittent, surface current with the corresponding strength and direction confirming the plausibility of the Ombai Jet [J. Sprintall, personal communication concerning unpublished results].

3. Surface Trapped Tidal Velocities

Internal tides were generated in Ombai Strait (285-355 km) and propagated both into the strait and up the slope to the shallow water above the sill (shown for the M_2 constituent in Figure 3a). Over the sill the, the internal tides became trapped in the surface layer. Large major axes for the M_2 constituent in the upper ocean extended over 100 km away from

the Ombai Sill into the Banda Sea (Figure 3a). The S_2 response was similar to the M_2 response. However, the diurnal responses differed and were smaller in magnitude (Robertson and Field 2008).

To investigate fluctuations of the combined baroclinic tides, the standard deviations of the baroclinic anomalies were determined (Figure 3b), with the baroclinic anomaly defined as the perturbation of the 3-D velocities from the 2-D velocities (2-D velocities were subtracted from

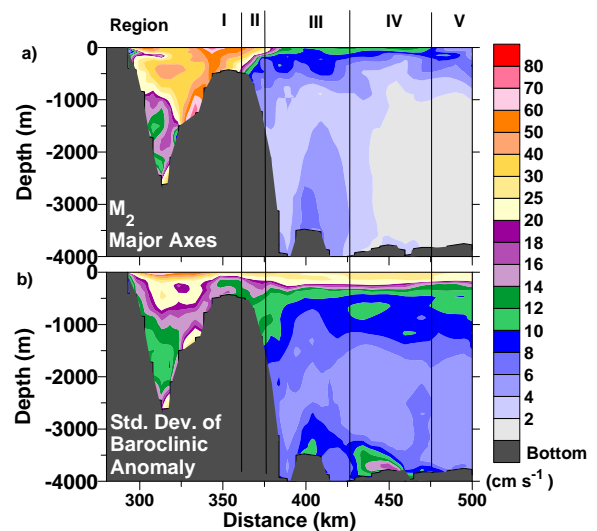


Figure 3. a) M_2 major axes of the tidal ellipses along transect through the east Ombai Strait region. b) The standard deviation of the baroclinic anomaly along the transect. The location of this transect is indicated in Figure 2. Regions III-V are in the Banda Sea.

the 3-D velocities removing the barotropic tidal response and isolating the baroclinic response). Since only tidal forcing was used in the model, the standard deviation of the baroclinic anomaly represents all resolvable fluctuations originating from tidal forcing. The standard deviation of the baroclinic anomaly showed a strong baroclinic response along the slope of the sill in the region of internal tide generation. Like the M_2 major axes, the combined baroclinic tidal response was trapped in the upper ocean extending well away from the sill.

To evaluate the spatial dependence of the response with the local topography and distance from the primary topographic feature, the Ombai sill, the transect was broken into five regions (Figure 3). Region I covered Ombai Strait and ran from 285-355 km (14 grid cells). Region II covered the slope northwest along the transect from 360-375 km (4 grid cells). The remaining regions, Regions III-IV, were located in deeper water of the Banda sea each progressively further along the transect (375-420 km, 425-470 km, and 475-520 km). Regions III-V had widths of 10 grid cells.

Internal waves universally in the ocean have been observed to follow the *Garrett and Munk (GM)* spectrum (Garrett and Munk, 1979), except in regions of internal wave generation. As a reference for the expected spectral slope and levels, *GM* spectra were determined following formula for horizontal velocities (Garrett and Munk 1979; Kanta and Clayson, 2000) for three different N values, $N = 5.0, 2.5,$ and 1.0 cph, representing the surface, the mid-water column, and the bottom, respectively (dashed lines in Figure 5 with the surface as cyan, mid-water column as red, and bottom as blue).

Horizontal velocity spectra were ensemble averaged for each of the five regions for three depths, surface, bottom, and a mid-depth level (level 12 out of 24), and are shown for the along-transect velocity in Figure 4. (Cross-transect velocity spectra are similar.) Spectra from the bottom and mid-depth agreed with the *GM* spectra both in level and slope in Region V, the furthest region away from the sill and the closest to background conditions. However, surface spectra (cyan) were well above *GM* spectral levels in all five

regions, reflecting an increase in energy in the upper ocean due to the baroclinic tides. In Regions I and II, where internal waves were generated in the deep portion between Timor Island and the sill and over the slope northwest of Ombai Sill, respectively, both spectral levels and spectral slopes deviated from the *GM* spectra (Figures 4a-b). This is particularly evident at frequencies between 3 and 8 cpd (Figures 4a-b). Pronounced peaks appeared at 4, 6, and 8 cpd in Region II corresponding to the overtides. The increases in spectral density at these high frequencies result from non-linear interactions between waves. Bispectra (not shown) confirmed transfer of energy from the tidal frequencies to these high frequencies, primarily from the semidiurnal tides. This indicated significant transfer of energy to higher harmonics in these regions. In Region I, spectral density levels at mid-depth (red) were equivalent to those at the bottom (blue), indicating intense activity throughout the water column. In the other regions, spectral densities were generally higher at the bottom (blue) than at the middle water column (red), indicating more intense benthic activity than in the mid-water column (Figure 4). In Region III, spectral slopes roughly followed *GM* (Figure 4c) and increases of spectral densities at high frequencies were slight, but noticeable. However, the spectral levels exceeded the *GM* levels, with the *GM* spectra falling outside the 95% confidence levels at high frequencies. In Regions IV and V, spectral levels agreed with both *GM* levels and slope with the *GM* spectral falling within the 95% confidence levels for these spectra (not shown). Thus, the spectra follow the expected *GM* relationship only in mid-depth and benthic layers in the deep basin regions well away from the topographic features generating the internal tides. In the other regions, internal tides propagating away from the generation sites increased the velocities in the upper ocean. In the two regions of active baroclinic tidal generation, the *GM* relationship did not hold and there was a significant generation of overtides and increase of spectral energy at high frequencies. Finally, surface trapping increased the spectral levels at the surface for all regions, even over 100 km away from generation site.

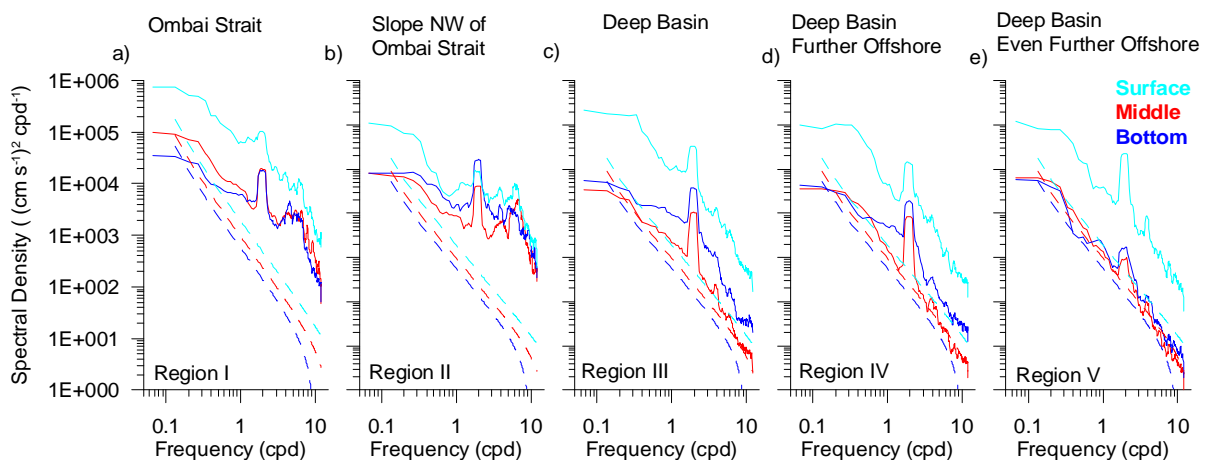


Figure 4. Ensemble averaged spectra of the surface (cyan), mid-water column (red), and bottom (blue) levels velocities for the five regions along the Ombai Strait transect. *Garrett-Munk* spectra are shown as dashed lines for the surface (cyan, $N=5.0$ cph), mid-water column (red, $N=2.5$ cph), and bottom (blue, $N=1.0$ cph).

4. Tidal Mixing

The intense upper level internal wave activity was associated with strong mixing. Internal tides commonly distorted the isotherms by 50-100 m. Temperature differences during 20 days exceeded 0.5°C in the upper 500 m, with the greatest temperature differences in the upper 200 m over the top of the sill and southeast into Ombai Strait. Heat was lost in the upper 100 m and gained at a depth ~ 250 m indicating a vertical mixing and a transfer of heat across the thermocline. Since solar radiation was not included in the simulations, unrealistic cooling of the surface occurred as the surface waters mixed with the cooler waters below and surface temperatures were not restored by incoming solar radiation. Temperature fluctuations were strongest in the same region, where standard deviations of potential temperature reached 2.0 °C, indicating strong isotherm fluctuations. The model represents vertical mixing through the vertical diffusivity, which was determined by the Generic Length Scale parameterization (Robertson and Ffield 2008). Over the Ombai Sill, extremely high vertical diffusivities of temperature and momentum, $> 0.5 \text{ m}^2 \text{ s}^{-1}$ occurred even in 15 day averages. Away from the sill, diffusivities were low, less than $1.0 \times 10^{-4} \text{ m}^2 \text{ s}^{-1}$. Intense mixing occurred in local regions such as over the sill and in the region of intense internal tidal activity (Regions I and II). Little mixing appeared to occur elsewhere and diffusivities elsewhere were low, less than $1.0 \times 10^{-4} \text{ m}^2 \text{ s}^{-1}$. At the sites of intense mixing, the diffusivities exceeded those of Hautala *et al.* (1996), $1.0 \times 10^{-4} \text{ m}^2 \text{ s}^{-1}$; however, their estimates are integrated along a flow path including both quiet patches and patches of intense mixing. Their method did not identify locations of high mixing such as sills; whereas our results show local patches of intense mixing in a background of low mixing. Diffusivity observations by Alford and Gregg (1999) in the upper 300 m of the Banda Sea agreed with our model results, both with levels of $K_p = 1.0 \times 10^{-6} \text{ m}^2 \text{ s}^{-1}$. Unfortunately, since the observations were made in a quiet region well away from topography, they are insufficient as a definitive verification of the model results. The model is capable of identifying locations of intense mixing due to internal tides. Much of the mixing in the Indonesian Seas is believed to occur in these sites of intense mixing, with the mixed fluid flowing from these regions according to its density.

5. Summary

Tides were found to have strong surface effects near Ombai Strait with development of the Ombai Jet and strong mixing in the upper water column. The Ombai Jet has implications for navigation and ship traffic. Since it is easily predictable, vessels can take advantage of it or avoid it to save fuel and time, which is useful, especially in times of high fuel prices. Internal tides were also found to be surface trapped in the region of Ombai Strait, influencing the upper ocean over 100 km away from the rough topographic feature generating the internal tide. Since most of the Indonesian Seas fall within 100 km of a rough topographic feature (Robertson and Ffield 2008), tides have the potential to affect surface velocities and mixing throughout the region. Mixing was found to be localized to intense mixing sites, which occurred in regions of high internal tidal activity and over

topographic features, such as the sill. In these areas, density diffusivities were extremely high, $K_p = 0.5 \text{ m}^2 \text{ s}^{-1}$, much higher than the background values of $K_p = 1.0 \times 10^{-4} - 1.0 \times 10^{-6} \text{ m}^2 \text{ s}^{-1}$. Thus, intense tidal-induced mixing over the sills and topographic features contributes significantly to the mixing of the Indonesian "Mix-Master". Larger scale models have not identified these features. Previous studies have shown that a resolution of 5 km or higher is required for baroclinic tidal simulations (Holloway and Merrifield 1999; Robertson 2006). Thus, there is a need for regional, fine-resolution tidal simulations in order to replicate features of this type. This brings out the question of what portion of the baroclinic tides, the coarse resolution global tidal simulations are capable of reproducing and how much of the actual tidal response they miss.

6. Acknowledgments

Funding for this work has been provided by U. S. Office of Naval Research through grant N00014-03-1-0423.

7. References

- Alford, M. H., M. C. Gregg, and M. Ilyas 1999: Diapycnal Mixing in the Banda Sea: Results of the First Microstructure Measurements in the Indonesian Throughflow, *Geophys. Res. Lett.* 26, 741-2744.
- Egbert, G. D., and S. Erofeeva 2002: Efficient inverse modeling of barotropic ocean tides, *J. Atmos. Oceanic. Tech.*, 19, 22,475-22,502.
- Ffield, A., and A. L. Gordon 1992: Vertical mixing in the Indonesian Thermocline, *J. Phys. Oceanog.*, 22, 186-195.
- Ffield, A., and A. L. Gordon 1996: Tidal mixing signatures in the Indonesian Seas, *J. Phys. Oceanog.*, 26, 1924-1935.
- Garrett, C. 2003: Internal tides and ocean mixing, *Science*, 301, 1858-1859.
- Garrett, C., and W. Munk 1979: Internal waves in the ocean, *Ann. Rev. of Fluid Mech.*, 11, 339-369.
- Gordon, A. L. 2005: Oceanography of the Indonesian Seas and their Throughflow, *Oceanography*, 18, 14-27.
- Hatayama, T. 2004: Transformation of the Indonesian throughflow water by vertical mixing and its relation to tidally generated internal waves, *J. of Oceanog.*, 60, 569-585.
- Hatayama, T., T. Awaji, and K. Akitomo 1996: Tidal currents in the Indonesian Seas and their effect on transport and mixing, *J. Geophys. Res.*, 101, 12,353-12,373.
- Hautala, S., J. Reid, and N. Bray 1996: The distribution and mixing of Pacific water masses in the Indonesian Seas, *J. Geophys. Res.*, 101, 12,375-12,389
- Holloway, P. E., and M. A. Merrifield, 1999: Internal tide generation by seamounts, ridges, and islands, *J. Geophys. Res.*, 104, 25,937-25,951.
- Kantha, L. H., and C. A. Clayson 2000: Numerical models of oceans and oceanic processes, Academic Press, San Diego, CA, 940 pp..
- Mazzega, P., and M. Bergé 1984: Ocean tides in the Asian semienclosed seas from TOPEX/POSEIDON, *J. Geophys. Res.*, 99, 24,867-24,881.
- Ray, R. D., G. D. Egbert, and S. Erofeeva 2005: Brief overview of tides in the Indonesian Seas, *Oceanography*, 18, 74-79.
- Robertson, R. 2006: Modeling Internal Tides over

Fieberling Guyot: Resolution, Parameterization, Performance, *Ocean Dynamics*, doi 10.1007/s10236-006-0062-5.

Robertson, R. and A. Field 2008: Baroclinic tides in the Indonesian Seas. Part 2: Interactions between tidal constituents, energy fluxes, and tidal mixing with a focus on Ombai Strait, doi:10.1029/2007JC004677.

Sprintall, J., S. Wijffels, A. L. Gordon, A. Field, R. Molcard, R. D. Susanto, I. Soesilo, J. Sopaheluwakan, Y. Surachman, and H. M. van Aken 2004: INSTANT: A new international array to measure the Indonesian Throughflow, *Eos Trans. AGU*, 85, Sept. 28, 369-376.

Susanto, R. D., A. L. Gordon, J. Sprintall, and B.

Herunadi 2000: Intraseasonal variability and tides in Makassar Strait, *Geophys. Res. Lett.*, 27, 1499-1502.